DOI: 10.1002/adma.200601221

Manipulating Magnetoresistance Near Room Temperature in $La_{0.67}Sr_{0.33}MnO_3/La_{0.67}Ca_{0.33}MnO_3$ Films Prepared by Polymer Assisted Deposition**

By *Menka Jain*,* *Piyush Shukla*, *Yuan Li*, *Michael F. Hundley*, *Haiyan Wang*, *Stephen R. Foltyn, Anthony K. Burrell, Thomas M. McCleskey, and Quanxi Jia**

Doped manganites, $RE_{1-x}A_xMnO_3$ (RE = rare-earth and A = alkaline-earth elements), have attracted much attention because of their potential applications in magnetic sensors and other devices.[1–5] A prominent feature of these materials is a metallic-insulating (MI) transition associated with the ferromagnetic–paramagnetic (FM–PM) transition.[4] The figure of merit of these colossal magnetoresistance (CMR) materials for many applications is the magnetoresistance ($MR = (\rho_H - \rho_0)/\rho_0$, where ρ_H and ρ_0 are the resistivities with and without a magnetic field, respectively). For practical applications, it is important to obtain a high MR at room temperature and at low magnetic fields. It has been observed that the MR near or at the transition temperature, T_c, for a given field strength, is generally larger for samples with lower T_c.[2] Thus, simply changing the composition of these manganites is not effective in obtaining large MR values near room temperature.

Many recent efforts in searching for enhanced MR have been focused on transport properties across artificial grain boundaries and interfaces by making FM manganite/spacer superlattices and FM–insulator–FM tunneling junctions.[6–8] However, the enhancements of the MR were mostly achieved at low temperatures (< 150 K). There have been only a few successful efforts to substantially enhance the MR values above 200 K. For example, Venimadhav et al. achieved a maximum MR of −98 % (with magnetic fields of 6–7 T) at 220 K in the $La_{0.67}Ca_{0.33}MnO_3/Pr_{0.70}Ca_{0.30}MnO_3$ superlattice prepared by pulsed laser deposition (PLD).[9] Sirena et al. observed an MR value of −18 % at 2 T around 280 K in the $La_{0.55}Sr_{0.45}MnO_3/La_{0.67}Ca_{0.33}MnO_3$ films prepared by sputtering.[10] Recently, an MR value of −60 % at a field of 8 T was reported at 270 K in a $La_{0.67}Sr_{0.33}MnO_3/Nd_{0.67}Sr_{0.33}MnO_3$ multilayer grown by PLD.[5]

In this work, we report our efforts to obtain a large MR near room temperature by preparing multilayer-coated $La_{0.67}Sr_{0.33}MnO_3/La_{0.67}Ca_{0.33}MnO_3$ (LSMO/LCMO) films using polymer assisted deposition (PAD). PAD is a solution technique that has been successfully used to prepare both simple and complex metal oxide films.[11,12] The LSMO and LCMO compounds have similar lattice parameters and have a Curie temperature above and below room temperature, respectively, which makes them very attractive for preparing multilayers.

The PAD technique was used to prepare the solutions of $La_{0.67}Sr_{0.33}Mn$ and $La_{0.67}Ca_{0.33}Mn$. These solutions were spin-coated onto single-crystalline (001) $LaAlO_3$ (LAO) substrates. After each coating, the films were heated at 600 °C for 5 min. For all the films, a total of 10 coatings were applied on the substrate and final annealing was performed at 950 °C for 2 h in oxygen. The thicknesses of the films were ca. 130 nm. Our initial study focused on optimizing the LSMO/LCMO ratio to get a maximum MR close to room temperature. The films with LSMO/LCMO volume ratios of 70:30, 60:40, and 50:50 had MR values of −61 %, −63 %, and −57 %, respectively, at 300 K at an applied field of 5 T. Hence, in this work we prepared multilayer-coated films by holding the LSMO/LCMO volume ratio constant (60:40 with maximum MR) and changing the number and the thickness of the individual layers. Details of the layered configuration with their sample identifications (ML1 and ML2) are illustrated in Figure 1. To make a direct comparison of the multilayer-coated films, a single-phase film of $La_{0.67}Sr_{0.198}Ca_{0.132}MnO_3$ (LSCMO), which is a uniformly mixed phase of the LSMO/LCMO at a volume ratio of 60:40, was also prepared under similar conditions.

In the X-ray diffraction (XRD) θ–2θ scans, only (00l) peaks of the multilayer-coated films and LAO substrate were observed, suggesting that the films had a preferential c-axis orientation. The (00l) peaks of the multilayer-coated films were asymmetric at 2θ angles between the (00l) peaks of LSMO and LCMO films. In other words, the (002) peak of the pure LSMO and LCMO (Fig. 2a) can be fitted with a single sym-

[*] Dr. M. Jain, Dr. Q. X. Jia, Y. Li, Dr. H. Wang, Dr. S. R. Foltyn
Superconductivity Technology Center
Materials Physics and Applications Division
Los Alamos National Laboratory
Los Alamos, NM 87545 (USA)
E-mail: mjain@lanl.gov; qxjia@lanl.gov
Dr. P. Shukla, Dr. A. K. Burrell, Dr. T. M. McCleskey
Materials Chemistry, Materials Physics and Applications Division
Los Alamos National Laboratory
Los Alamos, NM 87545 (USA)
Dr. M. F. Hundley
Condensed Matter and Thermal Physics
Materials Physics and Applications Division
Los Alamos National Laboratory
Los Alamos, NM 87545 (USA)

[**] This work was supported as a Directed Research and Development Project at Los Alamos National Laboratory under the United States Department of Energy.

ADVANCED MATERIALS

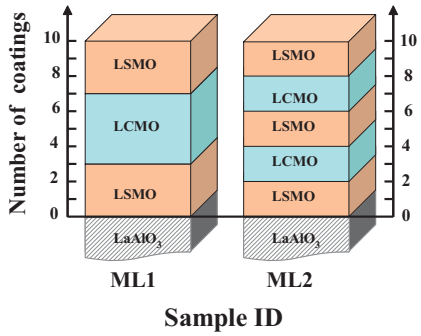

Figure 1. Schematic diagram of the multilayer-coated LSMO/LCMO films and sample identifications.

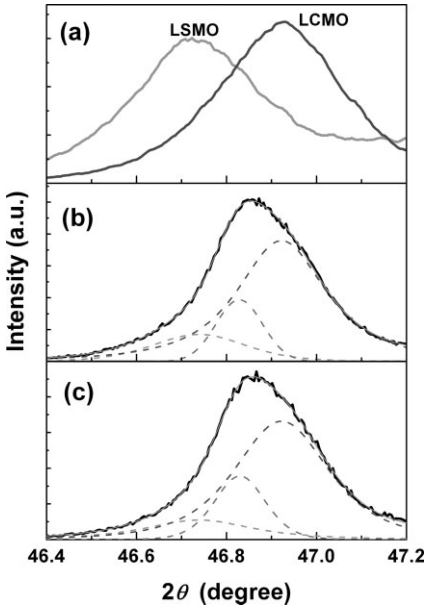

Figure 2. The (002) peak in the θ–2θ scans of a) pure LSMO and LCMO films, b) film ML1, and c) film ML2. The asymmetric (002) peaks of film ML1 and ML2 were well fitted with three peaks. The dashed lines show the three fittings.

metric peak with certain 2θ values. However, the asymmetric (002) peak of the multilayer-coated films can only be fitted with three symmetric peaks each (shown in dashed lines in Fig. 2b and c). In this case, two fittings are fixed at the 2θ values of the pure LSMO and LCMO films and the third one has no fixed parameters. This third peak was assumed to be due to the interfacial reaction that can lead to the formation of $La_{0.67}(Sr_{1-x}Ca_x)_{0.33}MnO_3$ phases. The relative net area under the third peak (for mixed phases) was observed to be greater in sample ML2 than sample ML1, which may be because of more interfaces in sample ML2 compared to sample ML1. The ϕ-scans (not shown here) were performed on reflections of the film {220} and the LAO {220}. The scan for films had four diffraction peaks with an average value of full width at half maximum of ca. 0.97° as compared to an average value of 0.6° for that of the LAO substrate. These results indicate that the films were of good epitaxial quality. Cross-sectional transmission electron microscopy (TEM) analysis (not shown here) of the ML2 sample taken from the <1$\bar{1}$2> zone shows that the interface between the film and the substrate is flat, without any visible secondary phases. The corresponding selected area diffraction (SAD) pattern taken from the interface area is shown in Figure 3. Distinguishable diffraction dots from the film indicate the high crystallinity of the film. The orientation relations between the film and the substrate, deduced from

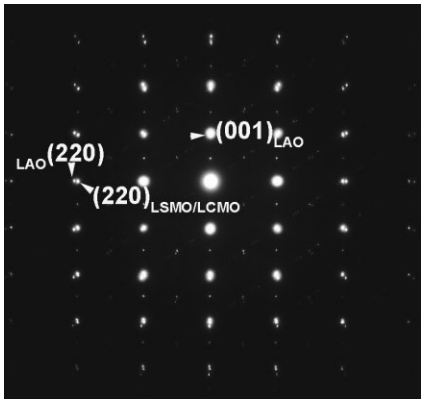

Figure 3. Selected area diffraction pattern from the interface area of the ML2 film.

both the SAD and XRD patterns, are $(220)_{film}//(220)_{substrate}$, $(001)_{film}//(001)_{substrate}$, and $[1\bar{1}2]_{film}//[1\bar{1}2]_{substrate}$. The (220) film plane aligned well with the (220) LAO plane. This is consistent with the small lattice mismatch observed from the SAD analysis.

Figure 4a shows the normalized resistivity, $\rho(T)/\rho(5\ K)\Delta$, of the multilayer-coated films and the LCSMO film along with that of LCMO and LSMO films. The absolute values of ρ at 5 K for the films LCMO, ML1, ML2, LSMO, and LCSMO were 0.68, 0.35, 0.16, 2.2, and 3.23 mΩ cm, respectively. The relatively lower ρ (as compared to LSMO) in the multilayer-coated films may come from the parallel connection of LCMO and LSMO or some intermediate phases at the interfaces. It is interesting to notice that a single MI transition peak is observed in the ρ versus temperature (T) curve of all the films. This behavior is in contrast with the double peak observed for the multilayered films prepared by PLD using different CMR materials.[13] In the PLD process, films are usually deposited at high temperature, and a sharp interface is expected. However, in the PAD process, low-temperature pyrolysis was carried out after each coating and a high-temperature annealing was employed only after the deposition of all layers. This "bottom-up" approach for epitaxial multilayer films may lead to a diffused or gradient interface, resulting in a single broad transition peak in the ρ versus T characteristics. These results support our XRD analysis where a single and asymmetric (002) peak was observed. The temperature at

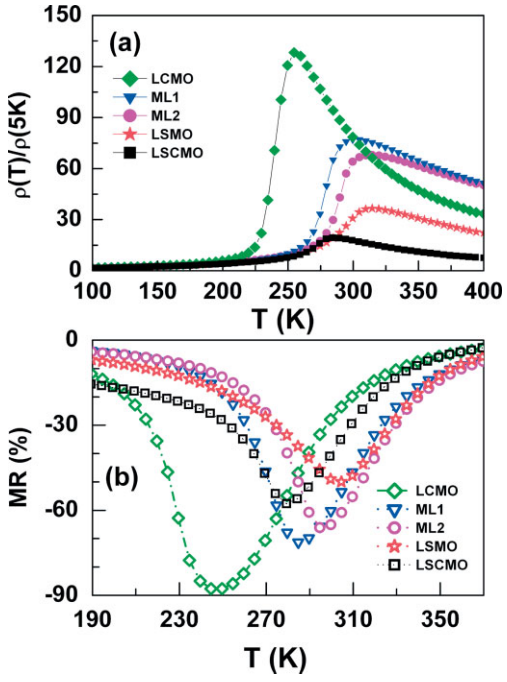

Figure 4. a) Normalized resistivity as a function of temperature for the multilayer-coated LSMO/LCMO films (ML1 and ML2) along with that of the pure LSMO, LCMO, and LSCMO films; and b) the temperature dependent magnetoresistance (at 5 T) for different films.

which the maximum resistivity occurs, T_p, of the ML1 and ML2 films is closer to that of the pure LSMO film,[12] which could be because of the presence of LSMO as the top layer or the larger LSMO/LCMO volume ratio. The T_p for the films coincides well with the Curie temperature (T_c) for the films, which shows the resistivity–magnetization correlation in these films.[1,4] The ρ(T) data in the temperature range 0–185 K can be fitted well by the form $\rho(T) = \rho_0 + \rho_1 T^2$, where the term $\rho_1 T^2$ represents electron–electron (e–e) scattering.[14–16] The coefficient ρ_1 for the films ML1 and ML2 is 2.88×10^{-8} and 1.43×10^{-8} $\Omega\,cm\,K^{-2}$, respectively. In the paramagnetic phase ($T > T_c$), the zero-field ρ of the films follows closely the law predicted by the small-polaron transport.[2,15,16] Fitting the experimental results yielded activation energies in the range of 77–100 meV for the multilayered films. The observed activation energies of single-phase LCMO and LSMO films are typically in the range of 70–150 meV.[12,15]

The MR values for the films were calculated from the resistivities at zero field and at different applied magnetic fields. At a low field of 0.5 T, multilayer-coated films ML1 and ML2 showed MR values of −4 % and −15.5 %, respectively, at 300 K. The MR values at an applied field of 5 T for all the films are plotted as a function of temperature in Figure 4b. Below 200 K, the MR was ca. −5 % at 5 T for multilayer-coated films, which indicates that there was no obvious grain-boundary effect.

It would be interesting to determine whether or not the enhanced MR near room temperature for our multilayer-coated films is mainly from the intermixing of two phase materials. To this end, we compared the MR values (at 5 T) of the multilayer-coated, LSCMO, LCMO, and LSMO films, as shown in Figure 4b. It is observed that the maximum MR (MR_{max}) values of −71 % (at 285 K) for multilayer-coated film ML1 and −66 % for ML2 (at 295 K) were much higher than the MR value of −58 % (at 280 K), obtained for single-phase LSCMO. At 300 K, the MR values for the ML1, ML2, and LSCMO films were −60 %, −65 %, and −41 %, respectively. These results clearly indicate that simply mixing LSMO with LCMO phases at a given volume ratio does not lead to the same properties as the multilayer-coated films. It should also be noted that most of the superlattice or multilayered manganite films with enhanced MR values reported in the literature were prepared by PLD, whereas the films in this study were prepared by a simple solution technique.

In summary, multilayer-coated LSMO/LCMO films were prepared using cost-effective PAD. The number of layers and individual layer thicknesses were varied while the LSMO/LCMO volume ratio was kept constant (60:40). Maximum MR values as high as −71 % and −66 % at 5 T were obtained at 285 K and 295 K, respectively. For comparison, a film of single-phase $La_{0.67}Sr_{0.198}Ca_{0.132}MnO_3$, which is a uniformly mixed phase of the LSMO/LCMO at a volume ratio of 60:40, was also prepared under similar conditions. The single phase $La_{0.67}Sr_{0.198}Ca_{0.132}MnO_3$ film shows a maximum MR of −58 % at 280 K. These results clearly indicate that the transition temperature (or temperature of maximum MR) and the magnitude of the MR can be manipulated through multilayer coating of two ferromagnetic materials. Similar properties could not be achieved by simply mixing LSMO with LCMO phases at the same volume ratio.

Experimental

Sample Preparation: Separate precursors were prepared using high purity (>99.99 %) metal salts ($La(NO_3)_3$, $Sr(NO_3)_3$, $MnCl_2$, and $Ca(OH)_2$). Water used in the solution preparation was purified using the Milli-Q water treatment system. Polyethyleneimine (PEI) was purchased from BASF Corporation of Clifton, NJ, and used without further purification. Ultrafiltration was carried out using Amicon-stirred cells and 3000 molecular weight cut-off, flat cellulose filter disks (YM3) under 60 psi (1 psi = 6.89 kPa) nitrogen pressure. Metal analysis was conducted on a Varian Liberty 220 inductively coupled plasma–atomic emission spectrometer (ICP-AES), following the standard SW846 EPA (Environmental Protection Agency) Method 6010 procedure.

First, $La(NO_3)_3 \cdot 6H_2O$ (5.73 mmol) was dissolved in 40 mL H_2O. Ethylenediaminetetraacetic acid (EDTA) (5.82 mmol) was added, followed by PEI (4.32 g) to prepare the lanthanum precursor. Similarly, $Sr(NO_3)_3$ (11.9 mmol) and EDTA (12.0 mmol) were stirred in 40 mL H_2O, and PEI (3.54 g) was added to make the strontium precursor. For making the manganese precursor, $MnCl_2 \cdot H_2O$ (11.8 mmol) and EDTA (5.82 mmol) were stirred in 40 mL of H_2O, and PEI (1.8 g) was added. The calcium precursor was prepared by stirring $Ca(OH)_2$ (4.20 mmol) in 40 mL H_2O and adding PEI (1.15 g). All these solutions were placed separately in an Amicon filtration unit and washed twice with H_2O. The final concentrations of La, Sr, Mn, and Ca in the precursors were 95, 274, 216, and 184 mM, respectively. These solutions were mixed in the required stoichiometric ratios to prepare solutions of $La_{0.67}Sr_{0.33}Mn$ and $La_{0.67-}$

ADVANCED MATERIALS

$Ca_{0.33}Mn$. These solutions were spin-coated onto the single-crystalline $LaAlO_3$ (LAO) substrate. For all the films, final annealing was performed at 950 °C for 2 h in oxygen.

Sample Characterizations: X-ray diffraction (XRD) was used to determine the film quality and orientation relationships between the film and the substrate. The microstructures of the selected film were also investigated by selected area diffraction (SAD), and cross-sectional transmission electron microscopy (TEM) using a JEOL-3000F analytical electron microscope. The resistivity (ρ) of the films was measured using a standard four-probe technique as a function of temperature (5–400 K) with different magnetic fields (0–5 T). For the ρ measurements, the magnetic field was applied perpendicular to the substrate surface.

Received: June 6, 2006

[1] A. P. Ramirez, *J. Phys.: Condens. Matter* **1997**, *9*, 8171.

[2] M. F. Hundley, M. Hawley, R. H. Heffner, Q. X. Jia, J. J. Neumeier, J. Tesmer, J. D. Thompson, X. D. Wu, *Appl. Phys. Lett.* **1995**, *67*, 860.

[3] M. Paranjape, A. K. Raychaudhuri, *Solid State Commun.* **2002**, *123*, 521.

[4] C. Zener, *Phys. Rev.* **1951**, *81*, 440.

[5] S. Mukhopadhyay, I. Das, *Appl. Phys. Lett.* **2006**, *88*, 032 506.

[6] a) L. M. B. Alldredge, Y. Suzuki, *Appl. Phys. Lett*. **2004**, *85*, 437. b) H. Li, R. Sun, H. K. Wong, *Appl. Phys. Lett.* **2002**, *80*, 628.

[7] J. Fontcuberta, M. Bibes, B. Martinez, V. Trtik, C. Ferrater, F. Sanchez, M. Varela, *J. Magn. Magn. Mater.* **2000**, *211*, 217.

[8] C. Kwon, K. C. Kim, M. C. Robson, J. Y. Gu, M. Rajeswari, T. Venkatesan, R. Ramesh, *J. Appl. Phys.* **1997**, *81*, 4950.

[9] A. Venimadhav, M. S. Hegde, R. Rawatb, I. Dasb, M. E. Marssic, *J. Alloys Compd.* **2001**, *326*, 270.

[10] M. Sirena, N. Haberkorn, L. B. Steren, J. Guimpel, *J. Appl. Phys.* **2003**, *93*, 6177.

[11] Q. X. Jia, T. M. McCleskey, A. K. Burrell, Y. Lin, G. E. Collis, H. Wang, A. D. Q. Li, S. R. Foltyn, *Nat. Mater.* **2004**, *3*, 529.

[12] M. Jain, P. Shukla, Y. Li, M. F. Hundley, M. Hawley, B. Maiorov, I. H. Campbell, L. Civale, A. K. Burrell, T. M. McCleskey, Q. X. Jia, *Appl. Phys. Lett.* **2006**, *88*, 232 510.

[13] E. S. Vlakov, K. A. Nenkov, T. I. Donchev, A. Y. Spasov, *Vacuum* **2003**, *69*, 255.

[14] a) A. Urushibara, Y. Moritomo, T. Arima, A. Asamitsu, G. Kido, Y. Tokura, *Phys. Rev. B: Condens. Matter Mater. Phys.* **1995**, *51*, 14 103. b) S. V. Pietambaram, D. Kumar, R. K. Singh, C. B. Lee, V. S. Kaushik, *J. Appl. Phys.* **1999**, *86*, 3317.

[15] a) D. Emid, T. Holstein., *Ann. Phys. (N. Y.)* **1969**, *53*, 439. b) Y. Sun, X. Xu, L. Zheng, Y. Zhang, *Phys. Rev. B: Condens. Matter Mater. Phys.* **1999**, *60*, 12 317.

[16] G. J. Snyder, R. Hiskes, S. Dicarolis, M. R. Beasely, T. H. Giballe, *Phys. Rev. B: Condens. Matter Mater. Phys.* **1996**, *53*, 14 434.